Geophysical Research Letters

RESEARCH LETTER
10.1029/2022GL097766

Key Points:

- Effective climate sensitivity is larger (feedback more amplifying) for historical anthropogenic aerosol than greenhouse-gas (GHG) forcing in Coupled Model Intercomparison Project phase 6
- The key difference is that GHG forcing is global and aerosols are mainly extratropical (and aerosol hemispheric contrast unimportant)
- Extratropical forcing causes a shallower temperature response than tropical forcing, hence more amplifying cloud and lapse-rate feedbacks

Supporting Information:

Supporting Information may be found in the online version of this article.

Correspondence to:

P. Salvi,
pietro.salvi14@imperial.ac.uk

Citation:

Salvi, P., Ceppi, P., & Gregory, J. M. (2022). Interpreting differences in radiative feedbacks from aerosols versus greenhouse gases. *Geophysical Research Letters*, *49*, e2022GL097766. https://doi.org/10.1029/2022GL097766

Received 6 JAN 2022
Accepted 26 MAR 2022

Interpreting Differences in Radiative Feedbacks From Aerosols Versus Greenhouse Gases

Pietro Salvi[1], Paulo Ceppi[1], and Jonathan M. Gregory[2,3]

[1]Department of Physics & Grantham Institute, Imperial College London, London, UK, [2]National Centre for Atmospheric Science, University of Reading, Reading, UK, [3]Met Office Hadley Centre, Exeter, UK

Abstract Experiments with seven Coupled Model Intercomparison Project phase 6 models were used to assess the climate feedback parameter for net historical, historical greenhouse gas (GHG) and anthropogenic aerosol forcings. The net radiative feedback is found to be more amplifying (higher effective climate sensitivity) for aerosol than GHG forcing, and hence also less amplifying for net historical (GHG + aerosol) than GHG only. We demonstrate that this difference is consistent with their different latitudinal distributions. Historical aerosol forcing is most pronounced in northern extratropics, where the boundary layer is decoupled from the free troposphere, so the consequent temperature change is confined to low altitude and causes low-level cloud changes. This is caused by change in stability, which also affects upper-tropospheric clear-sky emission, affecting both shortwave and longwave radiative feedbacks. This response is a feature of extratropical forcing generally, regardless of its sign or hemisphere.

Plain Language Summary Understanding how the Earth's surface temperatures change in accordance with the anomalous energy flow into the system due to changes in greenhouse gases (GHGs) or anthropogenic aerosols is vital for predicting future temperature change. New data have made it possible to better calculate how efficiently the planet responds to temperature change (so as to return to energy equilibrium) for historical aerosols and GHGs. We find that the Earth requires greater surface temperature changes under aerosol climate forcing than it does for GHGs in order to balance out incoming and outgoing energy into the Earth system. By comparing with experiments that prescribe energy changes only outside the tropics, we find that the lower efficiency of aerosols in damping the radiative imbalance is related to their being mainly located away from the equator, unlike GHGs which are generally well mixed throughout the globe. This forcing away from the equator is tied to the vertical distribution of temperature changes. This distribution affects how efficiently surface temperature change leads to balancing the incoming and outgoing energy into the Earth system. Surface temperature can thus change differently for the same global average forcings.

1. Introduction

Global warming due to future emissions of greenhouse gases (GHGs) and other climate forcing agents has been understood in recent years in terms of the energy imbalance that these forcings cause in the Earth system, to which this system responds through changing surface temperatures. The usual interpretive model is $N = F - \alpha T$, where α is the climate feedback parameter, N top-of-atmosphere energy imbalance, T global mean surface temperature change and F effective radiative forcing (Ramaswamy et al., 2001) (Note: we have chosen the sign convention where a positive α implies an increased positive-upwards radiative response for increasing surface temperatures.). Although this is helpful and intuitive as a simple model, there are several complications when using it (Andrews et al., 2015; Knutti & Rugenstein, 2015; Sherwood et al., 2015).

While there are generally confirmed differences in the feedback parameter across models (Andrews et al., 2012; Becker & Wing, 2020; Zelinka et al., 2020), there is not a consensus on whether α depends on the different forcing agents that are relevant to past and future temperature changes. Comparing aerosols and GHGs, the two dominant historical forcing agents (Smith et al., 2020), several studies have found differences in feedbacks (Marvel et al., 2016; Shindell, 2014; Smith & Forster, 2021). Gregory et al. (2020) presented evidence for a difference in α between anthropogenic forcing (GHGs and aerosols) and natural forcing by volcanic aerosols. By contrast, Richardson et al. (2019) did not find significant differences among forcing agents, considering several models in the Precipitation Driver Model Intercomparison Project (PDRMIP) experiments. The focus of this study is the dependence of α on the nature of the forcing agent.

In the recently released data of the Coupled Model Intercomparison Project phase 6 (CMIP6), historical single-forcing experiments across several models have become available for analysis. These new experiments allow us to obtain the effective forcings for different agents, allowing us to accurately calculate the corresponding radiative feedbacks over the historical period. Previous work has found a dependence of these feedbacks on SST patterns (Andrews et al., 2015; Ceppi & Gregory, 2019; Zhou et al., 2017), which affect the radiation budget via changes in stability and clouds (Andrews et al., 2018). Following this reasoning, this work considers how historical greenhouse gas and aerosol forcing affect SSTs and stability, and how these in turn modulate the radiative responses.

2. Data and Methods

Data for several historical forcing experiments was obtained from the ESGF CEDA archive (esgf-index1.ceda.ac.uk) for seven models: CanESM5, CNRM-CM6-1, GISS-E2-1-G, HadGEM3-GC31-LL, IPSL-CM6A-LR, MIROC6, and NorESM2-LM. These experiments include a control (piControl) with constant preindustrial forcing agents as well as experiments both with coupled atmosphere-ocean models (AOGCMs) and with atmosphere models (AGCMs) given prescribed sea surface conditions, for historical GHGs, aerosols, and all historical forcings together. The experiments, models and variants used are detailed in Table S1 in Supporting Information S1. The historical single-forcing AOGCM experiments hist-aer and hist-GHG were performed for the Detection and Attribution Model Intercomparison Project (DAMIP; Gillett et al., 2016), while the AGCM piClim simulations are part of the Radiative Forcing Model Intercomparison Project (RFMIP; Pincus et al., 2016). Where possible, we chose variants with the same initialization (i1 variant label), physics and forcing definition as in piControl. We included all realizations that contained all of the required variables, and our results from each experiment of each model are ensemble averages. We calculated multi-model mean (MMM) values from the individual model ensemble averages, with equal weighting for each model.

We analyze the upward TOA radiative response R, the stability response S as measured by the estimated inversion strength (EIS; Wood & Bretherton, 2006), and the cloud-radiative effect (CRE), measured as the difference between all-sky and clear-sky downward fluxes. Prior to analysis, all fields were regridded to a common T42 grid (corresponding to a grid resolution of approximately 2.8° in longitude and latitude), using conservative remapping for radiative fluxes, and bilinear interpolation for other fields. Monthly fields were aggregated into annual averages.

In order to separate out the surface warming (or cooling) driven feedbacks from the forcing and associated rapid adjustments (Hansen et al., 1997; Sherwood et al., 2015), we use the results from the AGCM experiments with fixed sea surface temperatures through the following equation:

$$X_{\text{response}} = X_{\text{AOGCM}} - X_{\text{AGCM}}, \tag{1}$$

where X_{response} represents the response of the variable of interest X. Radiative feedbacks and other responses per unit global warming were calculated through linear least-squares regression of the desired variable against globally averaged surface air temperature. The regressions are performed across the full length of the historical period (years 1850–2014) for all experiments, despite the possible time-dependence of α (Gregory & Andrews, 2016; Gregory et al., 2020) which we do not study in this work. Note that the impact of short-lived volcanic forcing should be minimal on the historical feedbacks calculated over this long time period.

Global averages in this paper refer to area-weighted averages of the variables of interest, except for stability S where the average is taken over ocean regions 50°S–50°N. This choice follows Ceppi and Gregory (2019), who found EIS equatorward of 50° to be well correlated with the global radiative response R in observations and in two GCMs.

The confidence intervals for results derived from regressions combine two aspects of uncertainty. The first is the variability among different ensemble members, which we have calculated for each model as the variance across members of the historical experiment. This experiment was chosen since it generally had the most ensemble members, with the assumption that the magnitude of unforced variability is representative of other forcing scenarios. The second is the estimated error in the regression slope of the ensemble-averaged data. The combined error is calculated as the square root of the sum of variances from these two aspects of uncertainty and given as $\pm 1\sigma$ of the probability distribution.

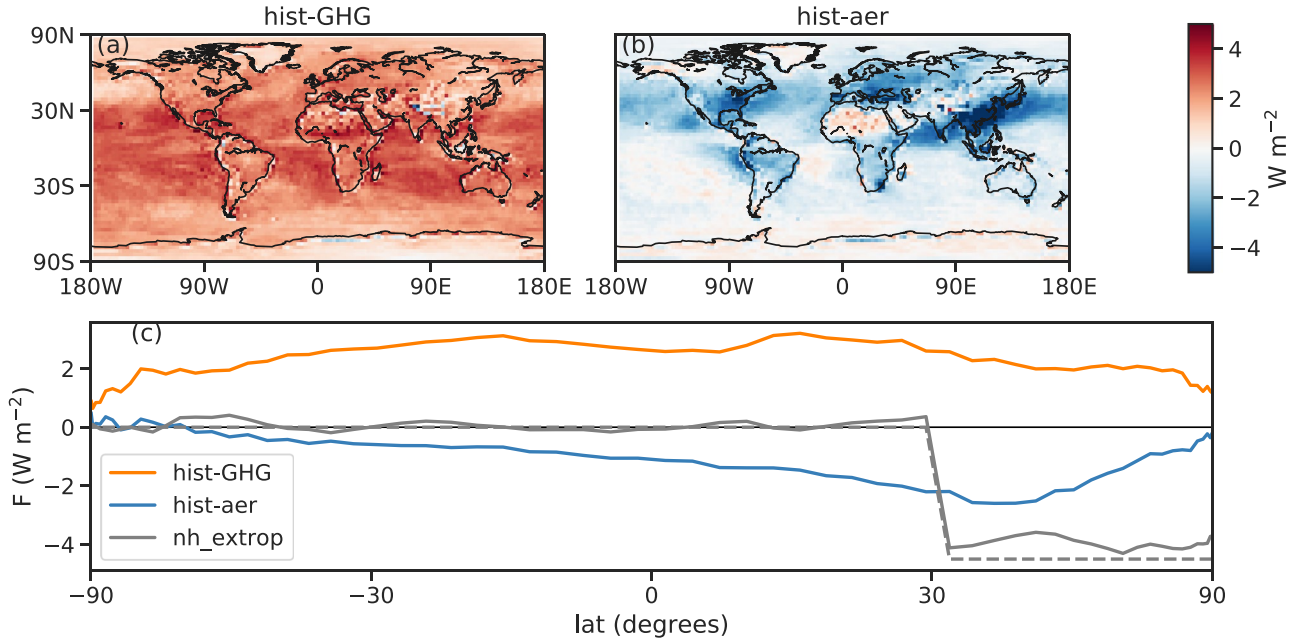

Figure 1. Top-of-atmosphere radiative forcing patterns over years 1995–2014 for hist-GHG (a) and hist-aer (b). The zonal-mean profiles of forcing are shown in (c), where values for hist-GHG (*orange*) and hist-aer (*blue*) are the average effective forcings of the relevant AGCM experiments (piClim-histghg and piClim-histaer, respectively) minus control. For nh_extrop (*gray*) the dashed line shows the prescribed instantaneous forcing whilst the solid line shows the effective forcing calculated from the HadAM3 (atmosphere-only) simulation. Note that the *x*-axis is scaled by geographical area.

Two idealized extratropical forcing experiments were run to investigate the impact of forcing localized away from the regions of deep convection on radiative feedbacks and tropospheric stability. These experiments are denoted as nh_extrop and sh_extrop for northern (30°N–90°N) and southern (30°S–90°S) hemisphere forcing, respectively. A uniform "ghost" radiative forcing of −4.5 W m^{-2} was imposed as an extra term in the surface energy budget in the relevant regions for each experiment. The imposed instantaneous radiative flux values were chosen so that the global average forcing would be comparable to that of hist-aer over years 1995–2014 (around − 1.13 W m^{-2}). Although the nh_extrop forcing is zonally uniform unlike the forcing for hist-GHG and hist-aer (Figures 1a and 1b), the nh_extrop setup was chosen to capture the skew of the northern extratropical forcing that is seen in hist-aer relative to the more homogeneous hist-GHG (Figure 1c). The idealized experiments were performed with the Hadley Centre Atmospheric Model version 3 (Pope et al., 2000) in both atmosphere-only (HadAM3) and slab ocean (HadSM3) configurations. The horizontal resolution is 2.5° × 3.75°; there are 19 levels in the atmosphere and the slab ocean has a thickness of 50 m. This model is one of the two used by Ceppi and Gregory (2019), and these experiments are the same as their − UNIF$_{ET}$ experiment for a single hemisphere at a time, except with a different forcing magnitude.

We also make use of tropical-only forcing experiments in HadSM3 and HadAM3 denoted as "tropical" in later figures. This is the same as the +UNIF$_{T}$ experiment in Ceppi and Gregory (2019), which involves a uniform forcing of 7 W m^{-2} over the tropics (30°S–30°N).

3. Investigating Radiative Feedback Differences in Terms of Stability Differences

The radiative feedbacks for historical aerosol and all historical forcings, relative to those from GHGs, are shown in Figure 2a, for each model analyzed and for the MMM. Colored bars show the all-sky net feedback parameter α, whilst markers show the CRE feedback parameter α_{CRE} (minuses) and clear-sky feedback parameter α_{CS} (pluses). In all cases, positive numbers mean less amplifying feedbacks, that is, a relatively larger upward radiative flux perturbation for positive *T*. The findings here show more amplifying feedbacks for hist-aer than hist-GHG in the MMM. On a model-by-model basis, hist-aer shows either significantly more amplifying or very similar feedbacks to hist-GHG (except for CNRM-CM6-1, the only model with a substantially less amplifying feedback for hist-aer). Neither α_{CS} (correlation of 0.80 with allsky α, Figure S1b in Supporting Information S1) nor α_{CRE}

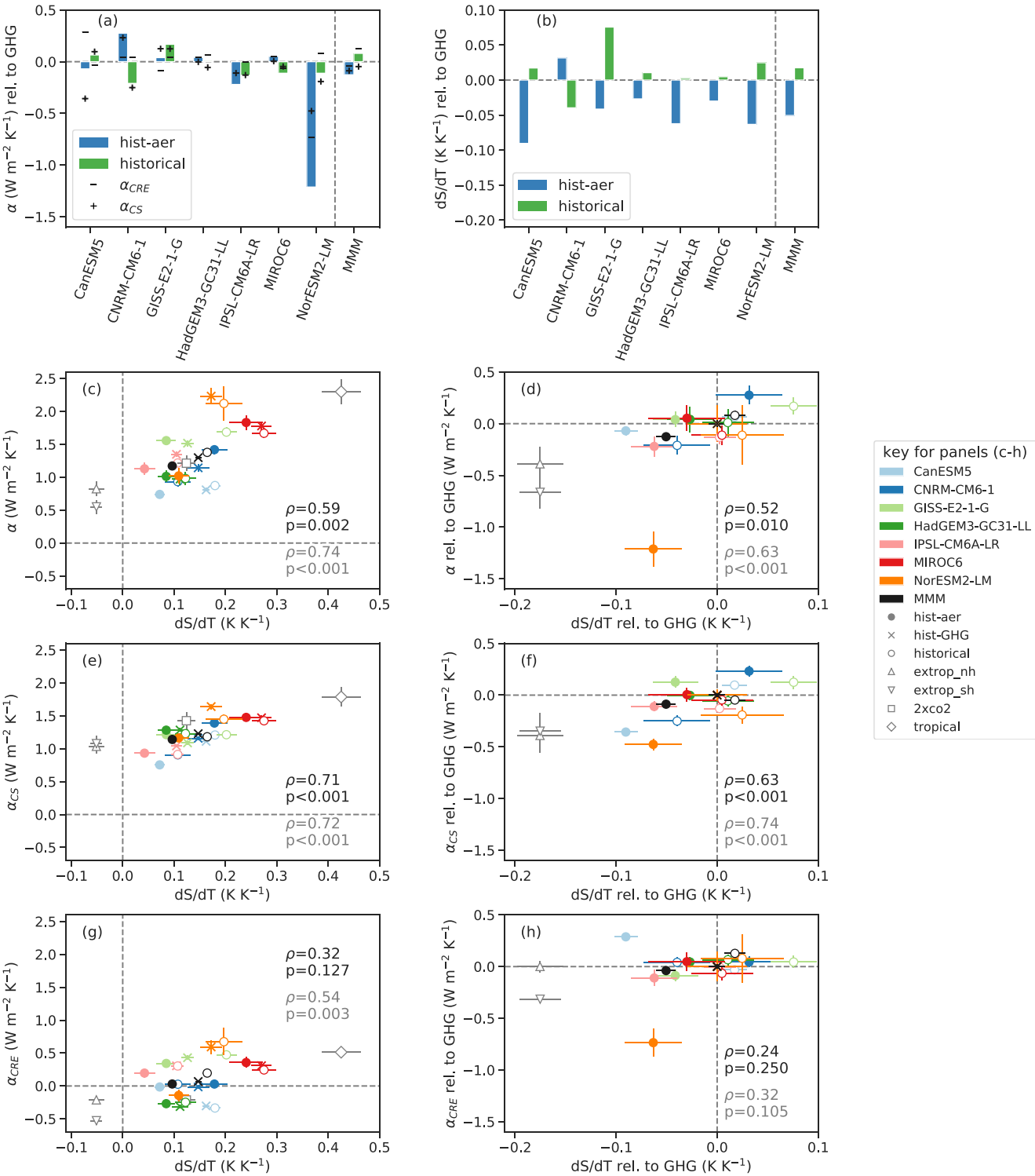

Figure 2. (a) All-sky radiative feedback parameter (α, *bars*) alongside cloud-radiative effect (CRE) (α_{CRE}, *minuses*) and clear-sky radiative feedback parameters (α_{CS}, *pluses*) for each model and the multi-model mean (MMM), as the difference from hist-GHG values. (b) Difference of dS/dT from hist-GHG values. (c, e, and g) Net (c) clear-sky, (e) CRE, and (g) all-sky radiative feedback parameters against net dS/dT. (d, f and h) as row above, except with values relative to hist-GHG. Confidence intervals in (c–h) denote ± one standard deviation based off combined regression and ensemble member uncertainties. The Pearson correlation ρ is shown in (c–h), across models and both excluding (*black*) and including (*gray*) the data points from the HadSM3 experiments. The tropical-only forcing experiment is included in (c, e, and g), as part of the inter-model trend, but excluded (both in plotting and ρ) in (d, f, and h) for clarity and to focus on the HadSM3 experiments that are more similar to hist-aer and hist-GHG. Also shown are p-values for the statistical significance of the correlations.

(correlation of 0.85 with allsky α, Figure S1d in Supporting Information S1) entirely explains the differences of all-sky α for aerosol (or the net historical forcing) compared to GHG forcing. Both correlations are highly significant ($p < 0.001$), which indicates that both clear-sky and CRE feedbacks are important in explaining the spread in α as neither α_{CS} nor α_{CRE} dominates the spread.

We propose that differences in radiative feedback across forcing agents may be explained in terms of different tropospheric stability responses and their impact on cloud and lapse-rate feedbacks. Figure 2b shows that hist-aer causes lower stability responses than hist-GHG across all models (except for CNRM-CM6-1). A greater increase in stability (as in GHG compared with aerosol) means more warming in the upper troposphere than at the surface, and hence a positive (less amplifying) lapse-rate feedback (Andrews & Webb, 2018; Ceppi & Gregory, 2019), with an additional minor contribution from relative humidity changes (Figure 6 in Ceppi & Gregory, 2019). Furthermore, tropospheric stability is a key variable for cloud formation, with higher stability encouraging the formation of low boundary-layer clouds over marine regions (Andrews & Webb, 2018; Ceppi & Gregory, 2019; Ceppi et al., 2017; Zhou et al., 2016). Low clouds have little impact on outgoing longwave radiation due to their temperatures being similar to those at the surface. Since they reflect incoming solar radiation, however, low clouds have an overall positive upwards (cooling) effect on radiation (Hartmann, 1994). Positive forcings that increase stability will thus tend to promote low-level cloudiness and give a positive upwards radiative feedback that opposes the forcing. The feedbacks from increased low cloud, combined with clear-sky feedbacks, are why we expect a positive correlation between net α and the stability response S per unit global warming, which we refer to as dS/dT.

Figure 2 (through its parts c–g) supports this. Considering all models and experiments together, there is a positive correlation between net α and dS/dT (0.59 for the AOGCM experiments, Figure 2c). Much of the spread in α among this set of models is related to stability, despite the implication of previous work that intermodel differences in climate feedback are dominated by cloud responses to mean SST warming (Ringer et al., 2014). This is still the case when feedbacks are broken down into α_{CS} (Figure 2e) and, although to a lesser extent, α_{CRE} (Figure 2g). We interpret the correlation in Figure 2e as being primarily driven by the linkage between stability and lapse-rate feedbacks (Andrews & Webb, 2018; Ceppi & Gregory, 2019).

By considering the difference in α between hist-aer and hist-GHG for each model, we remove part of the model spread in α , which affects both forcing agents equally, revealing the positive correlation (Figure 2d) between α and stability change in response to different forcing agents. Although the correlation across models is only moderate (0.52), it is nevertheless significant ($p = 0.010$), and the difference is also significant in the MMM according to estimated error bars. The lack of correlation in Figure 2h, both across models and in the MMM, despite such correlation in Figure 2f, suggests that the impacts of stability on clear-sky feedbacks are more robust than the impacts on α_{CRE} for explaining differences in α between historical aerosols and GHGs. This may be because the relationship between S and CRE is not consistently simulated among climate models. Alternatively, it is possible that, contrary to the findings of Ceppi and Gregory (2019), global stability changes are not strongly physically linked to CRE in some of the models, and that regional changes in S would be a better explanatory factor.

The historical all-forcing case is dominated by responses to GHGs and aerosols (Smith et al., 2020). Therefore, differences between historical and hist-GHG experiments are mostly due to differences between hist-aer and hist-GHG. Both the feedback parameter (Figure 2a) and the stability response (Figure 2b) are greater for historical than for hist-GHG in the MMM. This results from combining hist-GHG and hist-aer responses, given that aerosols and GHGs forcing are of opposite sign (Appendix B in the online supporting information of Gregory & Andrews, 2016). A visual explanation of it can be found in Figure S2 in Supporting Information S1.

The results here are in agreement with findings from previous studies of a greater transient climate response (indicative of a less positive α) from aerosols (Marvel et al., 2016) and extratropical forcing (Rose & Rayborn, 2016; Rose et al., 2014; Shindell, 2014) compared to forcing from well-mixed GHGs. By contrast, Richardson et al. (2019) found no significant differences in feedback between the two kinds of aerosols (SO_4 and BC) and GHGs, regardless of whether they calculated ERF as in the present paper, or additionally correcting for the impact of land surface temperature adjustments (Andrews et al., 2021). There are several possible explanations for our disagreement, including the following. (a) Despite its statistical significance, the difference we find between feedbacks to the aerosol and GHG forcing may be specific to our selection of models, which is smaller than theirs (7, vs. 11 in PDRMIP models). (b) Historical aerosol and the $5 \times SO_4$ forcing in PDRMIP might have important

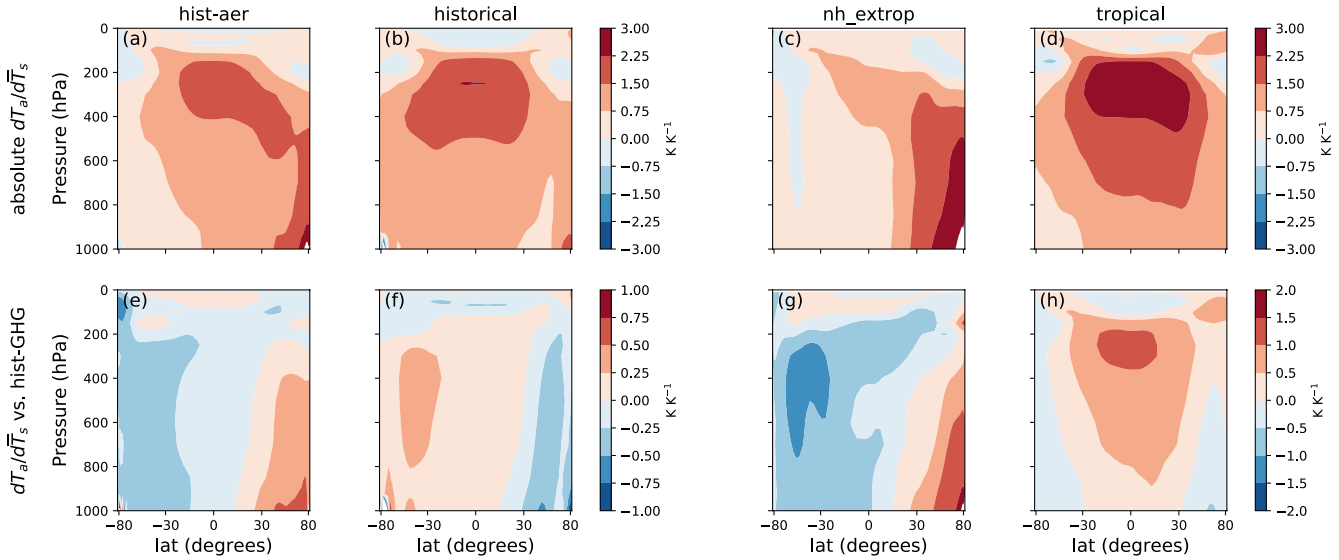

Figure 3. Multi-model mean (MMM) zonal-mean profiles of local air temperature regressed onto global-mean surface air temperature. Values shown are absolute (a–b), and relative to hist-GHG (e–f). Also shown are the results from the HadSM3 NH extratropical forcing (c) and tropical-only forcing (d), and these relative to the HadSM3 2 × CO_2 experiment (g–h). Note that the *x*-axis is scaled by geographical area.

differences in feedback, both because of different SO_4 concentrations and because of contributions of aerosols other than SO_4 (Myhre et al., 2014). (c) The step forcing experiments analyzed by Richardson et al. (2019) will be more representative of equilibrium responses than the historical simulations used here, which may affect the extent to which the feedbacks depend on the forcing agent.

4. Explaining Stability Differences in hist-aer in Terms of Extratropical Forcing

Next, we interpret the distinct radiative and stability responses to aerosols and GHGs in terms of the latitudinal distribution of forcing. Ceppi and Gregory (2019) demonstrated that positive tropical forcing tends to increase global stability per unit global surface warming, while positive extratropical forcing has the opposite impact (and vice versa for negative forcing). To understand why, we recall that the tropics are generally well coupled to the free troposphere, with the lapse rate closely following a moist adiabat due to moist convection (Flannaghan et al., 2014; Sobel, 2002). Consequently, tropical warming has a relatively large impact on free-tropospheric temperature. Mixing by atmospheric motions propagates the warming signal to the extratropical free troposphere, stabilizing the atmosphere there (Figures 3b and 3d). Conversely, positive forcing in the extratropics is expected to decrease stability, since surface temperature in the extratropics is more weakly coupled to the free troposphere. The effects of extratropical surface forcing tend to be more confined near to the surface (Figures 3a and 3c), and since this forcing acts on a region that is (on average) climatologically stable, the stability response is similar to that found for warming in other stable regions such as in the tropical South-East Pacific (Andrews & Webb, 2018). This effect can be seen by comparing air temperature changes in the hist-aer and hist-GHG cases (Figure 3e). (Note that aerosol forcing is *negative* and causes a surface *cooling*, but the patterns in Figure 3 are normalized by regression against global mean surface temperature change.)

This reasoning could explain why the hist-aer case gives a less positive stability response per unit surface warming than the hist-GHG case. The skew of forcing toward the extratropics in the hist-aer case (blue line in Figure 1c) means that a relatively larger fraction of the surface temperature response is in vertically decoupled regions, leading to the smaller dS/dT than in hist-GHG. In support of this hypothesis, we note that the pattern of tropospheric temperature change in the HadSM3 nh_extrop experiment compared to the 2 × CO_2 experiment (Figure 3g) is similar to the difference between hist-aer and hist-GHG (Figure 3e). The pattern from tropical-only forcing (Figure 3d) shows the propagation of warming to both the tropical and extratropical free troposphere in accordance with an increase to stability as seen in Figures 2c–2g, although stability is further increased over the tropics than in the more homogeneous 2 × CO_2 case (Figure 3h). Figure 2e shows that global-mean dS/dT is negative for both nh_extrop and sh_extrop, whereas it is positive in nearly every historical forcing experiment. This

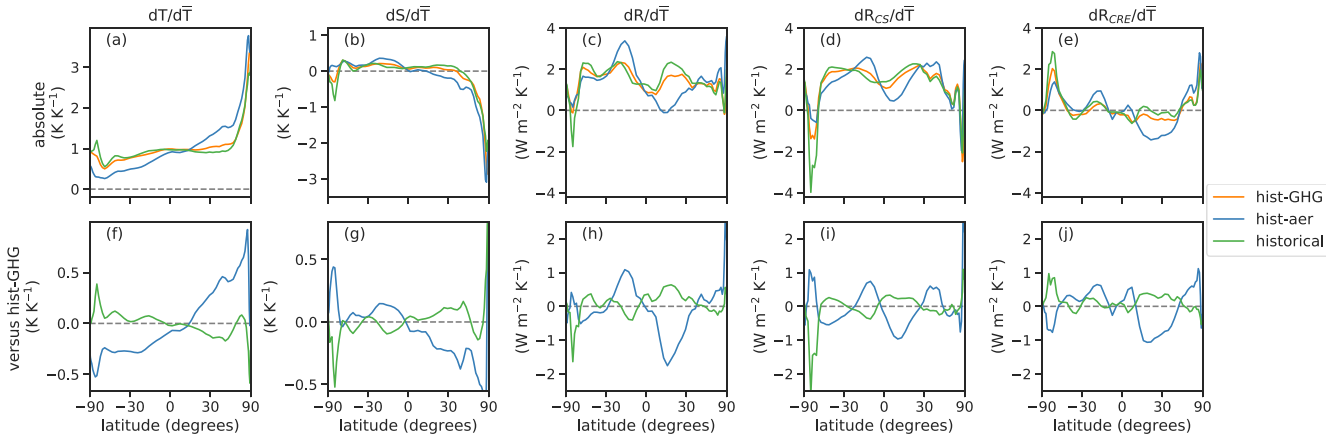

Figure 4. Multi-model mean (MMM) zonal-mean values regressed onto global-mean surface air temperature for the historical cases (*top* row) and differenced relative to hist-GHG (*bottom* row) in terms of (a and f) temperature, (b and g) estimated inversion strength, (c and h) net upwards radiative response, (d and i) upwards radiative response in clear sky and (e and j) upwards radiative response from cloud-radiative effect (CRE). Note that the *x*-axis is scaled by geographical area.

difference is probably related to the absence of tropical forcing in the idealized cases. That the negative d*S*/d*T* occurs for forcing in both hemispheres suggests that the essential characteristic is that the forcing is extratropical, rather than hemispheric. The historical all-forcing case shows the opposite pattern to hist-aer when compared to hist-GHG (Figures 3e and 3f), indicating that the aerosol has a similar effect on stability whether applied independently or jointly with GHGs.

To corroborate this reasoning, we consider the MMM zonal means of feedbacks and climate responses in Figure 4. There is less meridional contrast in response to hist-GHG than hist-aer (top row). Subtracting the responses from hist-GHG (bottom row), we see a positive NH temperature response per unit global warming in hist-aer relative to hist-GHG, and the opposite in the SH. This anticorrelates with the stability response per unit surface warming, which in turn correlates (in low latitudes) with the radiative response. The radiative response is then finally well explained, in terms of pattern, by the combination of clear-sky and CRE feedbacks.

Just as the global average feedbacks for the historical case are more positive than those for hist-GHG, the zonal-mean curves for hist-GHG generally lie between those for the net historical and hist-aer cases (top row of Figure 4), again consistent with the expected effect of aerosols. Likewise, the difference between historical and hist-GHG responses (bottom row of Figure 4) can be interpreted as representing the effect of aerosols, but with the sign reversed (see Text S1 in Supporting Information S1).

5. Summary and Conclusions

Our analysis of AOGCM historical experiments from CMIP6 (including new experiments which allow forcing to be diagnosed) reveals that climate feedback is more strongly amplifying (greater climate sensitivity) in response to anthropogenic aerosol forcing than greenhouse-gas (GHG) forcing. This difference is shown and is statistically significant in the MMM, though only seven AOGCMs have so far provided the required historical experiments and variables for this analysis, so it would be useful to repeat it with more. Our finding is consistent with those from past studies that also found greater climate sensitivity to aerosols than GHGs (Marvel et al., 2016; Shindell, 2014; Smith & Forster, 2021), but appears inconsistent with the recent study of Richardson et al. (2019). Further work is needed to explain the disagreement, which may relate to differences in the details of the prescribed aerosol forcing or the timescales of calculated feedbacks.

Furthermore, we find that the difference in (positive-stable) the net top-of-atmosphere radiative feedback parameter for aerosols and GHG forcing is positively correlated across AOGCMs with a difference in the response of tropospheric stability to the two kinds of forcing. We propose that the difference arises from the different latitudinal distributions of the forcing. An idealized slab model experiment with uniform surface forcing confined to the Northern extratropics qualitatively reproduces the near-surface extratropical temperature change that differentiates the historical aerosol experiment from the historical GHG experiment. The shallower extratropical

temperature change in the former is explained by the lower proportion of forcing in the tropics, where the surface is relatively strongly coupled to the free troposphere by deep convection (Flannaghan et al., 2014; Sobel, 2002), compared to the higher proportion of forcing in the extratropics, where the coupling is weaker and the effect of forcing more confined to the surface.

Thus a positive extratropical forcing causes a near-surface warming, which reduces tropospheric stability, whereas a positive tropical forcing has less effect on stability. A reduction in stability tends to reduce low-level cloudiness, which gives an anomalously negative (more amplifying) shortwave cloud feedback, whilst it also induces an anomalously negative clear-sky feedback. In this way, the latitude of forcing is linked to the radiative feedback it produces. Historical aerosol forcing is negative, so the signs of temperature and stability change are reversed, but the feedback parameter, sensitivity of stability (change per unit warming), and hence the correlation with the feedback parameter have the same sign for either sign of forcing: extratropical forcing tends to give higher climate sensitivity. This link accords with previous studies that have highlighted the impact of forcing patterns on radiative feedbacks (Ceppi & Gregory, 2019; Rose & Rayborn, 2016; Rose et al., 2014; Winton et al., 2010).

Historical climate change is dominated by GHG forcing. Hence the net feedback simulated in the historical experiments with all forcings is nearer to that for GHG than for anthropogenic aerosols. The effective climate sensitivity for historical forcing is slightly *smaller* than for historical GHG forcing (the magnitude of α is larger), because combining negative hist-aer forcing with positive hist-GHG forcing reduces the warming by more as a proportion than it reduces the net forcing, due to the greater sensitivity to aerosol forcing. We find also that some of the spread across AOGCMs in the climate sensitivity to GHG forcing is also correlated with the response of tropospheric stability to forcing; this aspect is intriguing and requires further investigation.

Data Availability Statement

Data that support the findings of this study are available online. The data from Coupled Model Intercomparison Project phase 6 (CMIP6) experiments can be found on the ESGF CEDA node available at esgf-index1.ceda.ac.uk. The data from the HadSM3 and HadAM3 experiments can be found at https://doi.org/10.6084/m9.figshare.17197748 and https://doi.org/10.6084/m9.figshare.17182907.

Acknowledgments
We thank two reviewers (Yuan-Jen Lin and anonymous) for constructive comments. P. Salvi was supported by the Department of Physics and the Grantham Institute of Imperial College London. P. Ceppi was supported by an Imperial College Research Fellowship and NERC grants NE/T006250/1 and NE/T007788/1. J. M. Gregory was supported by the European Research Council under the European Union's Horizon 2020 research and innovation programme (grant agreement No 786427, project "Couplet"). This work used JASMIN, the UK collaborative data analysis facility and the ARCHER UK National Supercomputing Service.

References

Andrews, T., Gregory, J. M., & Webb, M. J. (2015). The dependence of radiative forcing and feedback on evolving patterns of surface temperature change in climate models. *Journal of Climate*, *28*(4), 1630–1648. (Publisher: American Meteorological Society Section: Journal of Climate). https://doi.org/10.1175/JCLI-D-14-00545.1

Andrews, T., & Webb, M. J. (2018). The dependence of global cloud and lapse rate feedbacks on the spatial structure of tropical Pacific warming. *Journal of Climate*, *31*(2), 641–654. (Publisher: American Meteorological Society Section: Journal of Climate). https://doi.org/10.1175/JCLI-D-17-0087.1

Andrews, T., Gregory, J. M., Paynter, D., Silvers, L. G., Zhou, C., Mauritsen, T., et al. (2018). Accounting for changing temperature patterns increases historical estimates of climate sensitivity. *Geophysical Research Letters*, *45*(16), 8490–8499. https://doi.org/10.1029/2018gl078887

Andrews, T., Gregory, J. M., Webb, M. J., & Taylor, K. E. (2012). Forcing, feedbacks and climate sensitivity in CMIP5 coupled atmosphere-ocean climate models. *Geophysical Research Letters*, *39*(9). https://doi.org/10.1029/2012gl051607

Andrews, T., Smith, C. J., Myhre, G., Forster, P. M., Chadwick, R., & Ackerley, D. (2021). Effective radiative forcing in a GCM with fixed surface temperatures. *Journal of Geophysical Research: Atmospheres*, *126*(4), e2020JD033880. https://doi.org/10.1029/2020jd033880

Becker, T., & Wing, A. A. (2020). Understanding the extreme spread in climate sensitivity within the radiative-convective equilibrium model intercomparison project. *Journal of Advances in Modeling Earth Systems*, *12*(10), e2020MS002165. https://doi.org/10.1029/2020ms002165

Ceppi, P., Brient, F., Zelinka, M. D., & Hartmann, D. L. (2017). Cloud feedback mechanisms and their representation in global climate models. *Wiley Interdisciplinary Reviews: Climate Change*, *8*(4), e465. https://doi.org/10.1002/wcc.465

Ceppi, P., & Gregory, J. M. (2019). A refined model for the Earth's global energy balance. *Climate Dynamics*, *53*(7), 4781–4797. https://doi.org/10.1007/s00382-019-04825-x

Flannaghan, T. J., Fueglistaler, S., Held, I. M., Po-Chedley, S., Wyman, B., & Zhao, M. (2014). Tropical temperature trends in atmospheric general circulation model simulations and the impact of uncertainties in observed SSTs. *Journal of Geophysical Research: Atmospheres*, *119*(23), 13327–13337. https://doi.org/10.1002/2014jd022365

Gillett, N. P., Shiogama, H., Funke, B., Hegerl, G., Knutti, R., Matthes, K., et al. (2016). Detection and attribution model intercomparison project (DAMIP) (preprint). *Climate and Earth system modeling*. https://doi.org/10.5194/gmd-2016-74

Gregory, J. M., & Andrews, T. (2016). Variation in climate sensitivity and feedback parameters during the historical period. *Geophysical Research Letters*, *43*(8), 3911–3920. https://doi.org/10.1002/2016gl068406

Gregory, J. M., Andrews, T., Ceppi, P., Mauritsen, T., & Webb, M. J. (2020). How accurately can the climate sensitivity to CO_2 be estimated from historical climate change? *Climate Dynamics*, *54*(1), 129–157. https://doi.org/10.1007/s00382-019-04991-y

Hansen, J., Sato, M., & Ruedy, R. (1997). Radiative forcing and climate response. *Journal of Geophysical Research*, *102*(D6), 6831–6864. https://doi.org/10.1029/96jd03436

Hartmann, D. L. (1994). *Global physical climatology*. Academic Press.

Knutti, R., & Rugenstein, M. A. A. (2015). Feedbacks, climate sensitivity and the limits of linear models. *Philosophical Transactions of the Royal Society A: Mathematical, Physical & Engineering Sciences*, *373*(2054), 20150146. https://doi.org/10.1098/rsta.2015.0146

Marvel, K., Schmidt, G. A., Miller, R. L., & Nazarenko, L. S. (2016). Implications for climate sensitivity from the response to individual forcings. *Nature Climate Change*, *6*(4), 386–389. (Bandiera_abtest: a Cg_type: Nature Research Journals Number: 4 Primary_atype: Research Publisher: Nature Publishing Group Subject_term: Climate and Earth system modelling;Projection and prediction Subject_term_id: climate-and-earth-system-modelling;projection-and-prediction) https://doi.org/10.1038/nclimate2888

Myhre, G., Shindell, D., Bréon, F.-M., Collins, W., Fuglestvedt, J., Huang, J., et al. (2014). Anthropogenic and natural radiative forcing. In *Climate change 2013: The physical science basis. Contribution of working Group I to the fifth assessment Report of the Intergovernmental Panel on climate change*(Tech. Rep. No. AR5). Cambridge University Press. Retrieved from https://www.ipcc.ch/report/ar5/wg1/

Pincus, R., Forster, P. M., & Stevens, B. (2016). The radiative forcing model intercomparison project (RFMIP): Experimental protocol for CMIP6. *Geoscientific Model Development*, *9*(9), 3447–3460. https://doi.org/10.5194/gmd-9-3447-2016

Pope, V. D., Gallani, M. L., Rowntree, P. R., & Stratton, R. A. (2000). The impact of new physical parametrizations in the Hadley Centre climate model: HadAM3. *Climate Dynamics*, *16*(2), 123–146. https://doi.org/10.1007/s003820050009

Ramaswamy, V., Boucher, O., Haigh, J., Hauglustaine, D., Haywood, J., Myhre, G., et al. (2001). *Radiative forcing of climate change*. (Tech. Rep.). IPCC. Retrieved from https://www.ipcc.ch/site/assets/uploads/2018/03/TAR-06.pdf

Richardson, T. B., Forster, P. M., Smith, C. J., Maycock, A. C., Wood, T., Andrews, T., et al. (2019). Efficacy of climate forcings in PDRMIP models. *Journal of Geophysical Research: Atmospheres*, *124*(23), 12824–12844. https://doi.org/10.1029/2019jd030581

Ringer, M. A., Andrews, T., & Webb, M. J. (2014). Global-mean radiative feedbacks and forcing in atmosphere-only and coupled atmosphere-ocean climate change experiments. *Geophysical Research Letters*, *41*(11), 4035–4042. https://doi.org/10.1002/2014gl060347

Rose, B. E. J., Armour, K. C., Battisti, D. S., Feldl, N., & Koll, D. D. B. (2014). The dependence of transient climate sensitivity and radiative feedbacks on the spatial pattern of ocean heat uptake. *Geophysical Research Letters*, *41*(3), 1071–1078. https://doi.org/10.1002/2013gl058955

Rose, B. E. J., & Rayborn, L. (2016). The effects of ocean heat uptake on transient climate sensitivity. *Current Climate Change Reports*, *2*(4), 190–201. https://doi.org/10.1007/s40641-016-0048-4

Sherwood, S. C., Bony, S., Boucher, O., Bretherton, C., Forster, P. M., Gregory, J. M., & Stevens, B. (2015). Adjustments in the forcing-feedback framework for understanding climate change. *Bulletin of the American Meteorological Society*, *96*(2), 217–228. (Publisher: American Meteorological Society Section: Bulletin of the American Meteorological Society) https://doi.org/10.1175/bams-d-13-00167

Shindell, D. T. (2014). Inhomogeneous forcing and transient climate sensitivity. *Nature Climate Change*, *4*(4), 274–277. https://doi.org/10.1038/nclimate2136

Smith, C. J., & Forster, P. M. (2021). Suppressed late-20th century warming in CMIP6 models explained by forcing and feedbacks. *Geophysical Research Letters*, *48*(19), e2021GL094948. https://doi.org/10.1029/2021gl094948

Smith, C. J., Kramer, R. J., Myhre, G., Alterskjær, K., Collins, W., Sima, A., et al. (2020). *Effective radiative forcing and adjustments in CMIP6 models (preprint). Radiation/Atmospheric Modelling/Troposphere/Physics (physical properties and processes)*. https://doi.org/10.5194/acp-2019-1212

Sobel, A. H. (2002). The ENSO signal in tropical tropospheric temperature. *Journal of Climate*, *15*, 5. https://doi.org/10.1175/1520-0442(2002)015<2702:tesitt>2.0.co;2

Winton, M., Takahashi, K., & Held, I. M. (2010). Importance of ocean heat uptake efficacy to transient climate change. *Journal of Climate*, *23*(9), 2333–2344. (Publisher: American Meteorological Society Section: Journal of Climate) https://doi.org/10.1175/2009JCLI3139.1

Wood, R., & Bretherton, C. S. (2006). On the relationship between stratiform low cloud cover and lower-tropospheric stability. *Journal of Climate*, *19*(24), 6425–6432. https://doi.org/10.1175/jcli3988.1

Zelinka, M. D., Myers, T. A., McCoy, D. T., Po-Chedley, S., Caldwell, P. M., Ceppi, P., et al. (2020). Causes of higher climate sensitivity in CMIP6 models. *Geophysical Research Letters*, *47*(1), e2019GL085782. https://doi.org/10.1029/2019gl085782

Zhou, C., Zelinka, M. D., & Klein, S. A. (2016). Impact of decadal cloud variations on the Earth's energy budget. *Nature Geoscience*, *9*(12), 871–874. https://doi.org/10.1038/ngeo2828

Zhou, C., Zelinka, M. D., & Klein, S. A. (2017). Analyzing the dependence of global cloud feedback on the spatial pattern of sea surface temperature change with a Green's function approach. *Journal of Advances in Modeling Earth Systems*, *9*(5), 2174–2189. https://doi.org/10.1002/2017ms001096